

RSC Advances



This is an *Accepted Manuscript*, which has been through the Royal Society of Chemistry peer review process and has been accepted for publication.

Accepted Manuscripts are published online shortly after acceptance, before technical editing, formatting and proof reading. Using this free service, authors can make their results available to the community, in citable form, before we publish the edited article. This *Accepted Manuscript* will be replaced by the edited, formatted and paginated article as soon as this is available.

You can find more information about *Accepted Manuscripts* in the [Information for Authors](#).

Please note that technical editing may introduce minor changes to the text and/or graphics, which may alter content. The journal's standard [Terms & Conditions](#) and the [Ethical guidelines](#) still apply. In no event shall the Royal Society of Chemistry be held responsible for any errors or omissions in this *Accepted Manuscript* or any consequences arising from the use of any information it contains.

Preparation and characterization of PVDF/EG-POSS hybrid ultrafiltration membrane for anti-fouling improvement

Junfen Sun^{a*}, Lishun Wu^b, Fang Hu^a

- a. *State Key Laboratory for Modification of Chemical Fibers and Polymer Materials, College of Material Science and Engineering, Donghua University, North People Road 2999, Shanghai 201620, P. R. China*
- b. *Department of Chemistry and Chemical Engineering, Heze University, Daxue Road 2269, Heze, Shandong Province, 274015, P.R.China*

Corresponding Author: Junfen Sun, junfensun@dhu.edu.cn

Tel number: 86-18602105973, Fax number: 8621-67792855

Abstract: The Octa vinyl silsesquioxane (OvPOSS) was used to synthesis POSS grafted ethylene glycol (EG) (EG-POSS). EG-POSS was synthesized by a two-steps route. OvPOSS was first oxidized to prepare Epoxy-POSS. EG was used to graft Epoxy-POSS to obtain EG-POSS by ring opening reaction of epoxy groups. Polyvinylidene fluoride (PVDF)/EG-POSS hybrid membrane was prepared by phase separation process. POSS were characterized by FTIR, NMR and TEM. The hybrid membranes were characterized by pure water flux, retention ratio to BSA, contact angle, BSA adsorption capacity, mechanical property, XRD, SEM and AFM. The hydrophilicity and antifouling property of pure PVDF membrane was improved by incorporating EG-POSS. The pure water flux of hybrid membrane reached the maximum when 0.5% EG-POSS was added in the casting solution. The addition of EG-POSS had a positive effect on mechanical property of PVDF membrane.

Keywords: Polyvinylidene fluoride (PVDF); POSS; Hybrid ultrafiltration membrane; Ethylene glycol (EG)

1. Introduction

Poly(vinylidene fluoride) (PVDF) is a semi-crystalline polymer and is known for its thermo stability, aging resistance and chemical resistance to many acids and alkalis as well as good

biology and blood compatibility, which make PVDF as an attractive membrane material [1–3]. There are two main disadvantages for applying PVDF membrane. Fouling is one of major problems of PVDF membranes in water treatment application. The heavy membrane fouling happens when solutions containing substances like proteins are used to treat hydrophobic PVDF membrane. The other problem is the great shrinkage of wet PVDF membrane during drying process, thus the porosity and mean pore size would much be reduced [4,5]. So modification is very important in the PVDF membrane application. The general modify methods of PVDF are surface coating [6], surface grafting [7], plasma treatment [8], and blending [9]. Blending is a simple and the effective method to improve the properties of microporous membranes. In recent years, several polymers such as poly (acrylic acid) (PAA) [10], polyvinyl chloride (PVC) [11], poly(N- isopropylacrylamides) (PNIPAAm) [12], high-density polyethylene (HDPE) [13], polysulfone [14] and polyether sulfone [15], were blended with PVDF to prepare blending membranes. Besides inorganic particles such as SiO₂ [16], TiO₂ [17], Al₂O₃ [18], CaCO₃ [19] and Fe₂O₃ [20], were involved to modify PVDF membranes.

With the development of nanotechnology, the studies of hybrid membrane prepared with organic polymer and inorganic filler have attracted much attention. For hybrid membranes, the most commonly used nano inorganic filler includes nano zeolite [21], carbon molecular sieves [22], graphene oxide [23] and multi-walled carbon nanotubes (MWCNTs) [24]. As one type of porous nano-fillers, polyhedral oligomeric silsesquioxane (POSS) has attracted more and more interest in recent years due to its molecular-level mixing characteristics in the polymer matrix [25, 26]. POSS is an organic/inorganic hybrid material with a cage structure that comprises 6-12 silicon atoms together with oxygen atoms [27]. Different kinds of functional or nonfunctional organic groups are attached to the corner Si atom. The organic peripheral groups can vary depending on the purpose and application. These organic groups are divided into two categories: one is an inert group, such as cyclohexyl, cyclopentyl methyl, ethyl and so on; another is a reactive group, such as epoxy group, amino group and so on. POSS with active groups are suitable for polymerization, grafting or surface bonding [28]. Lee prepared Polyimide/POSS nanocomposites by copolymerization of octakis(glycidyl dimethylsiloxy)octasilsesquioxane (Epoxy-POSS), 4,4'-oxydianiline diamine (ODA), and 4,4'-carbonyldipthalic anhydride (BTDA) [29]. Choi prepared Cubic Silsesquioxanes and epoxy nanocomposites [30]. Lewicki

synthesized a series of partially opened POSS-diol cage (disilanolisobutyl POSS) and prepared POSS modified nanohybrid polyurethane elastomers [31].

POSS molecules could be incorporated into the polymer matrix to prepare hybrid membrane by different preparation methods such as co-polymerization or physical blending to improve thermal, mechanical and rheological properties. Recently hybrid membrane incorporating POSS has received substantial attention for various applications. Moon prepared polyamide-POSS hybrid membranes for seawater desalination [32]. Fu prepared polybenzimidazole (PBI)/POSS and polyacrylonitrile (PAN)/polyvinylpyrrolidone (PVP) dual-layer hollow fiber membranes for forward osmosis and osmotic power generation [33]. Tishchenko studied fouling behaviors of chitosan/POSS membranes to transport amino acids [34]. Chen prepared PBI/POSS/PAN hollow fiber membranes for engineering osmosis process [35]. Konietzny prepared polyimide/POSS hybrid membranes for the removal of sulfur aromatics by pervaporation [36]. Li prepared POSS-Matrimid-Zn²⁺ nanocomposite membranes for the separation of natural gas [27]. Recently poly(ethylene glycol) (PEG) was used to functionalize POSS and the composite membranes consisting of PEG functionalized POSS (PEG-POSS) were prepared by some researchers [37-41]. Rahman prepared PEBAX/ PEG-POSS nanocomposite membranes for CO₂ separation [42, 43]. Ethylene glycol (EG) is being widely used as the solvent, lubricants and surfactants in industries, and is being used as a component of cold-reserving materials and a component of nonfreezing coolants of automobiles for daily necessities [44]. EG as small molecular material and can modify POSS and improve the hydrophilicity of POSS easily compared to PEG. EG-POSS is a useful candidate to improve the hydrophilicity of hybrid membranes and compatibility between POSS and polymer matrix. The antifouling property and mechanical property of pure PVDF membrane can be improved by blending POSS and PVDF together to prepare hybrid membrane.

Nonetheless, less work has been done in PVDF/POSS hybrid membrane. In this work, Octa vinyl silsesquioxane (OvPOSS) was used to synthesis Epoxy-POSS. The epoxy groups of Epoxy-POSS were opened and grafted by ethylene glycol (EG) to prepare POSS grafted with EG (EG-POSS). The hybrid membrane including PVDF and EG-POSS were prepared by phase separation process.

2.Experimental

2.1. Materials

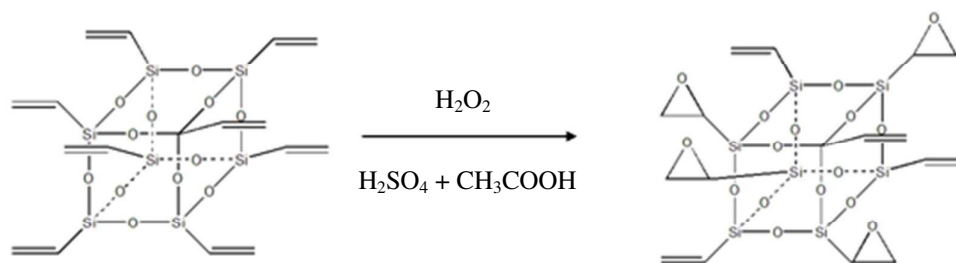
Octa vinyl silsesquioxane (OvPOSS, 99%) was purchased from Aladdin (China). The CHCl_3 (99%, AR), NaHCO_3 (AR), NaOH (CP), EG (AR) were purchased from Sinopharm Chemical Reagent Co. (China). CH_3COOH (99.5%, AR), H_2SO_4 (98%, AR), H_2O_2 (30%, AR) were bought from Jingke microelectronic materials Co. Ltd. (China). Polyvinyl pyrrolidone (PVP-K30 and PVP-K90) were purchased from BASF China Ltd. Polyvinylidene fluoride (PVDF 6020,CP) was bought from Solvay China Ltd. Dimethyl acetamide (DMAc, AR), alcohol (AR) and bovine serum albumin (BSA, Mw=67000) were obtained from Shanghai Chemical Reagent Company (China).

2.2. POSS modification and characterization

2.2.1 POSS modification

2.2.1.1 Synthesis of Epoxy-POSS

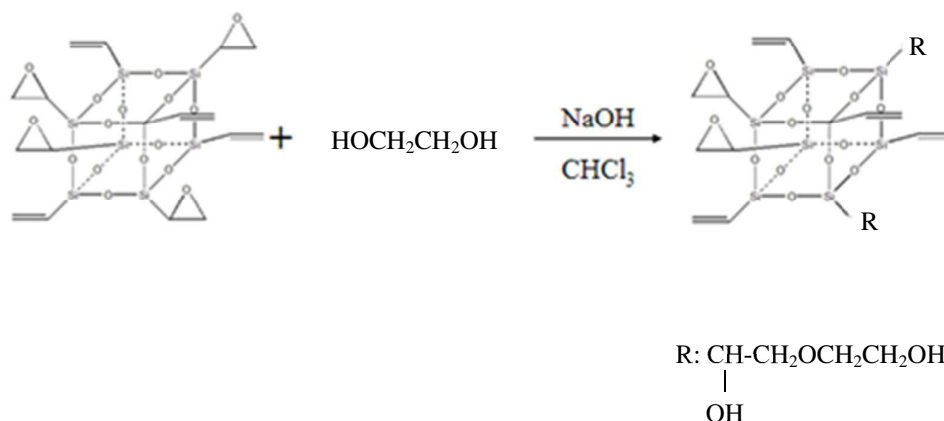
Epoxy-POSS was synthesized from OvPOSS through functional group conversion method. A three-necked flask was equipped with a magnetic stirrer. 6g OvPOSS, 110ml CHCl_3 , 25ml CH_3COOH and 0.8ml H_2SO_4 were added in a three-necked flask and heated to 60°C . 50ml H_2O_2 (30 wt%) was added in the mixed solution slowly. All the reaction was under a reflux atmosphere for 12 h. After the reaction was completed, a separate funnel was used to liquid separation, remove the upper layer. The sodium bicarbonate solution and deionized water were used to wash the lower layer several times. The resulting solution was ventilation volatilized at room temperature for 12 h, and then dried in a vacuum oven at 60°C . Epoxy-POSS was obtained and the yield was calculated.



2.2.1.2 Preparation of EG-POSS

0.7g Epoxy-POSS was dissolved in 10ml tetrahydrofuran (THF) in a three-necked flask. 20ml EG and 0.35ml 30% NaOH aqueous solution as a catalyst were added in the mixed solution separately. The mixture was stirred and refluxed at 35°C for 4h. The liquid in the three-necked flask was poured into a small beaker after the reaction completed. The beaker was put on a heating

apparatus to evaporate THF till the liquid turned into viscous material and then filtration was operated. The final product was put into a vacuum oven at 60°C for 24h.



2.2.2 Fourier transform infrared spectroscopy

The chemical and structural compositions of the samples were studied by a Nicolet 8700 Fourier transform infrared spectroscopy (FTIR) in the frequency range 4000 cm^{-1} -400 cm^{-1} . The samples were mixed with KBr powders and pressed into a disk suitable for FTIR measurement. The functional groups presented in the particles were characterized and identified by their peaks as obtained in the spectra.

2.2.3 Nuclear Magnetic Resonance

^1H -NMR spectra of the OvPOSS and the Epoxy-POSS were obtained on a Bruker Avance 400 (400 MHz) spectrometer at ambient temperature. Deuterated chloroform (CDCl_3) (0.03% v/v tetramethylsilane (TMS) in CDCl_3) was used as the solvent for all the samples in the Nuclear Magnetic Resonance (NMR) measurement. TMS was used as the internal standard.

2.2.4 Element analysis

The percentage contents of C, H, N in the OvPOSS and the Epoxy-POSS were determined by an Elemental Analyser (EA, Vario EL III, Elementar, Germany). The samples were dried under vacuum at the temperature of 60 °C for 24 h before measuring.

2.2.5 Transmission electron microscope

The size and morphology of particle were observed by using transmission electron microscope (TEM, JEM-2100F, JEOL, Japan). The samples were dried under vacuum at the

temperature of 60 °C for 24 h before measuring. The samples were put in chloroform to prepare 0.1 mg/ml solution and ultrasonically dispersed for 10 min. The solution was casted on a carbon coated copper grid and the samples were ready for observation after evaporation of the solvent.

2.3 Preparation and characterization of PVDF/EG-POSS hybrid membrane

2.3.1 Preparation of PVDF/EG-POSS hybrid membrane

The membranes used in this study were prepared by the phase inversion method. EG-POSS were dispersed into DMAc to prepared EG-POSS solutions and sonicated for 1 h until adequate dispersion was reached. After dispersing EG-POSS in solvent, PVDF and PVP were dissolved in the dope solutions by continuous stirring at 40°C for 1 h and 75°C for 24 h until homogeneous mixed solutions with various compositions were obtained. PVP were used as pore forming additives. The concentration of PVDF, PVP (K90) and PVP (K30) in DMAc is 15%, 3% and 3% respectively. The EG-POSS was added into the casting solution in order to improve membrane performance. The amount of EG-POSS is 0, 0.2, 0.5, 1.0, 1.5 and 2.0 wt% respectively in casting solution. The hybrid membranes were prepared by immersion precipitation. The polymeric mixture was cast on a glass plate and immediately immersed into water bath. The membranes formed a few moments after immersion. The hybrid membranes were washed with tap water at room temperature to remove residual solvent.

2.3.2 Scanning electron microscopy

For scanning electron microscopy (SEM), membranes were dried in air at room temperature and cryogenically broken in liquid nitrogen. The obtained cross-sections were dried overnight under vacuum at 30 °C and gold coated. The cross sections, as well as the top and bottom surfaces of the membrane were characterized by scanning electron microscopy (SEM, JSM-5600LV, JEOL, Japan).

2.3.3 X-ray diffraction

The crystal structures of membranes were detected by a wide angle X-ray diffraction instrument (WAXD) (XRD-6000, Shimadzu, Japan). The radiation source (Cu Ka X-ray) was operated at 40 kV and 30 mA, with the scanning angle ranging from 0° to 60°.

2.3.4 Atomic force microscopy

The roughness of membrane was determined by using an atomic force microscopy (AFM) (Veeco, Nanoscope IV, USA). Small squares of the membranes were cut and fixed on iron

substrate. The membrane surfaces were examined in a scan size of $5\mu\text{m} \times 5\mu\text{m}$. The membrane morphology was measured in the tapping mode. The roughness parameters of the membrane surface were assessed by software mathematical analysis. The surface roughness parameters were reflected in terms of the average roughness (Ra) and the root mean square of the Z data (Rq). Cross sections were prepared under cryogenic conditions with a Leica Cryo-Ultramicrotome EM UC7 equipped with a diamond knife.

2.3.5 Pure water flux

The membranes were subjected to pure water flux estimation at a trans-membrane pressure of 0.1MPa under cross-flow filtration. The permeability was measured under steady-state flow. Pure water flux was calculated as follows:

$$J_w = \frac{Q}{A\Delta t}$$

Where Q is the quantity of permeate collected (in l), and A is membrane area (m^2), Δt is the sampling time (h), J_w is pure water flux ($\text{l}\cdot\text{m}^{-2}\cdot\text{h}^{-1}$).

2.3.6 Shrinkage ratio, porosity and mean pore size

A number of wet membranes immersed in the water were cut into a_0 mm in length and b_0 mm in width. The length and width of membranes were measure by vernier caliper. The water of the membrane surface was absorbed by filter paper. The weight W_1 and thickness L of the wet membranes were measured by balance and spiralmicrometer. The membranes were dried at 60°C in an oven for 3 h. Then the lengths and widths of the membranes became a mm and b mm. The weight W_2 of the dry membrane was measured again. The shrinkage ratio ε was calculated by using the formula as follows:

$$\varepsilon = \left(1 - \frac{a \times b}{a_0 \times b_0}\right) \times 100\%$$

The porosity P of the membrane was calculated by the formula as follows:

$$P = \frac{W_1 - W_2}{\rho \cdot a \cdot b \cdot L} \times 100\%$$

The mean pore size R by water flowing velocity method was calculated by the following formula:

$$R = \sqrt{\frac{8\eta_{H_2O} \cdot J \cdot L}{P \cdot \Delta P}}$$

Where ρ is the density of the water, J is the pure water flux of the membrane, η_{H_2O} is the dynamic viscosity of the water, ΔP is the transmembrane pressure. [45]

2.3.7 Retention to BSA

The retention ratio of membranes was tested with 0.5mg/l BSA solution. The absorbances of original liquids and permeated liquids were determined with a UV-1800 spectrophotometer which was produced by SHIMADZU Company at the wavelength of 280nm. The retention ratio was derived as follows:

$$\text{Retention ratio (\%)} = \left(1 - \frac{2C_2}{C_0 + C_1}\right) \times 100\%$$

Where C_1 and C_2 are the concentrations of feeding solution and permeation solution after filtration respectively, and C_0 is the concentration of original feeding solutions.

2.3.8 Contact angle

The contact angle of the membranes was obtained on a OCA40 contact angle measuring instrument. The membranes were clipped into small pieces (1cm×6cm) and put in a vacuum oven at 30°C for 12h. Each sample was measured five different points, and the average data were taken as the sample's contact angle.

2.3.9 BSA adsorption capacity

The static protein adsorption capacity of membranes was determined with bovine serum albumin (BSA). The membranes were dried at 30°C in a vacuum oven before examination. The samples containing 2 g/l BSA were incubated with an exact amount of membranes in sealed containers under continuous shaking at 25°C. The membrane adsorbed the BSA thereby reducing the BSA concentration in the bulk. The equilibrium BSA concentration after 24 h was monitored in time with a UV-1800 spectrophotometer which was produced by SHIMADZU Company. The BSA depletion was measured at 280nm with 5mm quartz cuvettes.

2.3.10 Mechanical property

The mechanical property of membranes were tested by (WDW3020) at room temperature. The tensile ratio is 50mm/min. The length, width and thickness of membranes are 70mm, 15mm and 0.13mm respectively.

3. Results and discussion

3.1 Characterization of EG-POSS

Fig.1 shows $^1\text{H-NMR}$ spectra of the OvPOSS and Epoxy-POSS. Chemical shift of OvPOSS at 5.8-6.0ppm and 6.0-6.2ppm respectively corresponds to the hydrogen peak of $\text{CH}=\text{CH}_2$ and $\text{CH}=\text{CH}_2$, and the peak area proportion is 1:2 because of the coupling of the hydrogen atoms in $\text{CH}=\text{CH}_2$. Chemical shift of Epoxy-POSS at 2.24ppm, 2.80ppm and 2.93ppm reflect the hydrogen peak of epoxy group and the area is 1.8123, 2.0216 and 2.0967 respectively. The unoxidized hydrogen peak of $\text{CH}=\text{CH}_2$ is located in the vicinity of 6.0ppm and its area is 6.7669. It means the Epoxy-POSS is successfully synthesized and the epoxy concentration in Epoxy-POSS is 46.7%.

Fig. 2 illustrates FT-IR spectra of the OvPOSS, Epoxy-POSS and EG-POSS. The spectra of OvPOSS and Epoxy-POSS exhibit Si-O-Si stretching of the silsesquioxane cage at 1106 cm^{-1} . Compared to OvPOSS, the spectrum of Epoxy-POSS exhibits new peaks which refer to α C-H of epoxy group bending vibration peak at 1332 cm^{-1} and C-O symmetric and asymmetric stretching vibration peaks at 1234 cm^{-1} and 878 cm^{-1} . It implies that epoxy groups are successfully introduced into OvPOSS and the cage structure is not destroyed during the oxidation process. The new band at 1050 cm^{-1} appears at the spectrum of EG-POSS and is associated to C-O-C, which reveals that EG has been successfully grafted onto Epoxy-POSS. The intensity of peaks at 1332 cm^{-1} , 1234 cm^{-1} and 878 cm^{-1} at the spectrum of EG-POSS obviously decrease, which means just part of epoxy groups participate in the reaction. Table 1 shows the elemental content of Epoxy-POSS and EG-POSS. The percentage contents of C, H, N in the Epoxy-POSS and EG-POSS were shown in Table 1. The H content is almost same in Epoxy-POSS and EG-POSS, as shown in Table 1. During the reaction process from Epoxy-POSS to EG-POSS, the decrement of C content is same to the increment of O content because the Si content is always same. So EG-POSS concentration is 33.5% according to the data in Table 1.

Fig. 3 shows TEM micrographs of OvPOSS and EG-POSS. The dark spots are POSS particles. There are different grey colors as background in Fig. 3A and B because the thickness of carbon coating on the copper grid is not even. The size of OvPOSS and EG-POSS is close and uniform, and is about 3-4 nm, as shown in Fig. 3. It means the size of POSS does not change after modification process.

3.2 Characterization of PVDF/EG-POSS hybrid membranes

Fig.4 shows the cross section of pure PVDF membrane and PVDF/EG-POSS hybrid membranes. The pure PVDF membrane and PVDF/EG-POSS hybrid membranes possess similar sponge-like porous structure, as shown in Fig.4. However the pore size of hybrid membranes gradually decreases with increasing EG-POSS content, as shown in Fig.4. When EG-POSS content is 0.5%, the pore size of hybrid membrane is similar to that of pure PVDF membrane. When EG-POSS content is 1.0%, the pore size of hybrid membrane obviously decreases and the hybrid membrane is dense (Fig. 4C), which leads to lower pure water flux. It is suggested that increasing content of EG-POSS particles in casting solution accelerate the viscosity of casting solution and decreases the phase inversion speed and results in the formation of more small pores in hybrid membrane.

Fig.5 shows the surface structure of pure PVDF membrane and PVDF/EG-POSS hybrid membrane. The top surface and bottom surface of pure PVDF membrane are smooth, as shown in Fig. 5A1 and 5A2. The top surface and bottom surface of hybrid membrane embedded with 0.5% EG-POSS (Fig. 5B1 and 5B2) are similar to those of pure PVDF membrane. The top surface and bottom surface of hybrid membrane embedded with 1.0% EG-POSS (Fig. 5C1 and 5C2) are coarse compared to those of pure PVDF membrane and PVDF/EG-POSS hybrid membrane embedded with 0.5% EG-POSS. There are no obvious clusters or agglomerates on the surfaces of hybrid membranes. This shows the compatibility of EG-POSS particles with the polymer matrix.

Fig. 6 shows XRD patterns of PVDF/EG-POSS hybrid membranes embedded with different EG-POSS content. Table 2 shows crystallinity of hybrid membranes embedded with different EG-POSS content. XRD patterns of the membranes illustrates that the characteristic peaks of PVDF membrane are at 2θ of 18.4, 20.0, 29.5 and 40.3° . The characteristic peaks of PVDF/EG-POSS hybrid membranes at 2θ become weaker with increasing EG-POSS content in membrane, which indicates that crystallinity of hybrid membrane decreases with increasing EG-POSS content. The crystallinity of hybrid membranes embedded with different EG-POSS content shows this trend, as shown in Table 2 It is suggested that the addition of EG-POSS in the membrane depresses the crystallization of PVDF membrane.

The surface roughness of the membranes has significant effect on membrane fouling and

membrane with smoother surface often has better anti fouling characteristics. Fig. 7 shows AFM images of PVDF/EG-POSS hybrid membranes embedded with different EG-POSS content. Table 3 shows roughness parameters of PVDF/EG-POSS hybrid membranes embedded with different EG-POSS content. Ra, Rq and Rmax represent the average deviation of height, route mean square deviation of height and the maximum height. As shown in Table 3, Ra, Rq and Rmax of hybrid membrane with 0.5% EG-POSS changes less compared to those of pure PVDF membrane. Ra, Rq and Rmax of hybrid membrane with 1.0% EG-POSS decreases a lot compared to pure PVDF membrane and hybrid membrane with 0.5% EG-POSS. It is suggested that the roughness of hybrid membrane obviously decreases when more EG-POSS was added in the PVDF membrane. The effect of hydrophilicity of EG-POSS accelerates the exchange rate between solvent and non-solvent during the phase inversion, and the exchange rates increases with increasing EG-POSS content in hybrid membranes. In this case, the reorganization time of PVDF molecular chains on the surface of hybrid membrane becomes short, leading to formation of the hybrid membrane with smooth surface.

Fig. 8 shows AFM images of the cross section of PVDF/EG-POSS hybrid membranes embedded with different EG-POSS content. The EG-POSS appear as white spots in the AFM image. The brighter areas correspond to PVDF phase and the darker areas correspond to pores in hybrid membranes. The morphology of cross section of hybrid membranes embedded with different EG-POSS content is similar since the particle loading is not very high. The distribution of EG-POSS in hybrid membranes is good, as shown in Fig. 8 B and C. It is suggested that low content of EG-POSS can be evenly dispersed in the hybrid membranes and no clusters or agglomerates appear in the hybrid membranes. There are more pores in the hybrid membrane embedded with 0.5% EG-POSS (Fig. 8 B), which agrees well with the test of porosity of hybrid membranes.

3.3 Pure water flux, retention ratio, contact angle, porosity, pore size and shrinkage ratio

Fig. 9 presents pure water flux and retention ratio of PVDF/EG-POSS hybrid membranes embedded with different EG-POSS content. The pure water flux increases with increasing the content of EG-POSS and reaches the maximum when 0.5% EG-POSS is added in the hybrid membrane. The retention ratio to BSA decreases with increasing the content of EG-POSS and

reaches the minimum when 0.5% EG-POSS is added in the hybrid membrane. However the pure water flux decreases and retention ratio to BSA increases with further increasing the content of EG-POSS. The hydrophilicity of hybrid membrane increases with increasing the content of EG-POSS, which makes pure water flux increase with increasing the content of EG-POSS. At the same time low content of EG-POSS has less influence on the structure of hybrid membrane when the content of EG-POSS is lower than 0.5%. So the pure water flux reaches the maximum and the retention ratio reaches the minimum when 0.5% EG-POSS is added in the casting solution. However the structure of hybrid membrane become dense when the content of EG-POSS is more than 0.5%, which lead to low pure water flux and high retention ratio.

Fig.10 shows contact angle of PVDF/EG-POSS hybrid membranes embedded with different EG-POSS content. The contact angle of pure PVDF membrane is 83.1° . Contact angle decreases with increasing the content of EG-POSS. The contact angle is 75.0° when 2.0% EG-POSS is added in the casting solution. It means that the hydrophilicity of hybrid membrane is enhanced with increasing the content of EG-POSS. Through strong interfacial interaction with polymers, nano-particles blended in composite membranes help in shaping the morphology and property of membranes and in influencing the performance of membranes (hydrophilicity, flux and fouling resistance) by affecting the membrane interface behavior with water and/or foulants, in water treatment and industrial application [46].

Fig. 11 shows porosity, mean pore size and shrinkage ratio of PVDF/EG-POSS hybrid membranes embedded with different EG-POSS content. Porosity and mean pore size of hybrid membrane reach the maximum when 0.5% EG-POSS was added in the membrane, which corresponds to the change of pure water flux and retention ratio of hybrid membranes shown in Fig. 9. The shrinkage ratio decreases with increasing the content of EG-POSS and keeps stable when 1.0% EG-POSS was added in the membrane. It means that EG-POSS in membrane effectively inhibits the shrinkage of PVDF membrane. The entanglement between EG-POSS particles and PVDF molecular chains inhibits the organic shrinkage that occurred during the precipitation process of wet-casting polymeric membranes.

3.4 BSA adsorption capacity

Here BSA was used as a model protein to investigate the hydrophilicity and antifouling

property of hybrid membranes. Fig.12 shows BSA static adsorption capacity of PVDF/EG-POSS hybrid membranes embedded with different EG-POSS content. Pure PVDF membranes are easily contaminated by protein and other bio-molecules for its hydrophobicity as they are applied for microfiltration or ultrafiltration process. The BSA static adsorption capacity of pure PVDF membrane is 5.76 mg/g, as shown in Fig.12. It decreases with increasing the content of EG-POSS and reaches stable when the content of EG-POSS is more than 1.0%, about 2.61 mg/g. It is suggested that the hydrophilicity and antifouling property of pure PVDF membranes is effectively improved by incorporating EG-POSS in membranes.

3.5 Mechanical property

The introduced additives have different effects on the mechanical properties of the resultant membranes [47]. Xu reported that the mechanical strength of PVDF blend membranes was enhanced by adding appropriate amounts of O-MWCNT [47]. Li found that the addition of CaCO_3 had a negative effect on the mechanical strength of PVDF blend membrane [48]. Fig. 13 shows mechanical property of PVDF/EG-POSS hybrid membranes embedded with different EG-POSS content. The tensile strength of hybrid membrane increases gradually with increasing the content of EG-POSS when the content of EG-POSS is 0-1.5%, and decreases less when the content of EG-POSS is 2.0%. It is suggested that EG-POSS particles as additive improve mechanical property of PVDF membrane. This is the combined effects of solution viscosity and the dispersion of EG-POSS. The increased solution viscosity leads to a denser membrane structure which is beneficial for improving mechanical property of hybrid membranes with increasing the content of EG-POSS from 0-1.5%. After further increasing EG-POSS to 2.0%, the aggregation of EG-POSS and the weak interface compatibility between EG-POSS and hydrophobic PVDF matrix results in a decrease of mechanical property of hybrid membrane. Fig. 14 shows tensile stress-strain curves for hybrid membranes embedded with different EG-POSS content. The strain first increases and then decreases as EG-POSS increases in the hybrid membranes. The strain of hybrid membrane embedding with 2.0% EG-POSS decreases a lot and exhibits brittle behavior. From the stress-strain curves, it can be concluded that the hybrid membrane embedding with 1.5% EG-POSS processes the highest tensile stress.

3. Conclusions

POSS grafted ethylene glycol (EG) (EG-POSS) was synthesized and used as nanofiller in the preparation of PVDF/EG-POSS hybrid membrane. Embedding EG-POSS to PVDF matrix caused an increase in hydrophilicity and antifouling property of the membranes. The BSA static adsorption capacity of hybrid membranes decreases with increasing the content of EG-POSS and reaches stable when the content of EG-POSS is more than 1.0%. The permeability of hybrid membrane was dependent on the content of EG-POSS in the hybrid membrane. The pure water flux reaches the maximum and the retention ratio reaches the minimum when 0.5% EG-POSS is added in the casting solution. The addition of EG-POSS has a positive effect on mechanical property of PVDF membrane. The hybrid membrane can be applied for antifouling membrane.

Acknowledgements

The authors thank National Natural Science Foundation of China (51203020); Scientific Research Starting Foundation for Returned Overseas Chinese Scholars, Ministry of Education of China.

Reference

- [1] S. Munari, A. Bottino, G. Capannelli, *J. Membr. Sci.* 16 (1983) 181.
- [2] T.H. Young, L.P. Cheng, D.J. Lin, et al., *Polymer* 40 (1999) 5315.
- [3] D. Duputel, E. Staude, *J. Membr. Sci.* 78 (1993) 45.
- [4] D.L. Wang, K. Li, W.K. Teo, *J. Membr. Sci.* 178 (2000) 13.
- [5] K. Jian, P.N. Pintauro, *J. Membr. Sci.* 135 (1997) 41.
- [6] J. Hou, G. Dong, Y. Ye, V. Chen, *J. Membr. Sci.* 469 (2014) 19.
- [7] Q. Li, H.-H. Lin, X.-L. Wang, *Membranes* 4 (2014)181.
- [8] C. Yang, X.-M. Li, J. Gilron, D.-F. Kong, Y. Yin, Y. Oren, C. Linder, T. J. He, *Membr. Sci.* 456 (2014) 155.
- [9] X.-R. Meng, H.-Z. Zhang, L.Wang, X.-D. Wang, D.-X. Huang, *Desalin. Water Treat.* DOI: 10.1080/19443994.2014.926648
- [10] Y. He, X. Chen, S. Bi, C. Shi, L. Chen, L. Li, *Polym Advan. Technol.* 24 (2013) 934.
- [11] Q. Zhang, S. Zhang, Y. Zhang, X. Hu, Y. Chen, *Desalin. Water Treat.* 51 (2013)3854.
- [12] X. Chen, S. Bi, C. Shi, Y. He, L. Zhao, L. Chen, *Colloid Polym. Sci.* 291 (2013) 2419.
- [13] H. Liu, J. Liu, Q. Zhou, J. Wang, *Mater. Lett.* DOI: 10.1016/j.matlet.2013.03.033
- [14] Q. Chen, Z. Cui, J. Li, S. Qin, F. Yan, J. Li, *J. Power. Sources.* 266 (2014) 401.
- [15] L. Wu, J. Sun, Q. Wang. *J. Membr. Sci.* 285 (2006) 290.
- [16] S.-H. Zhi, J. Xu, R. Deng, L.-S. Wan, Z.-K. Xu, *Polymer (United Kingdom)* 55 (2014) 1333.
- [17] J. Hou, G. Dong, Y. Ye, V. J. Chen, *J. Membr. Sci.* 469 (2014) 19
- [18] X.S. Yi, S.L. Yu, W.X. Shi, S. Wang, N. Sun, L.M. Jin, C. Ma, *Desalination* 319 (2013) 38.
- [19] B. Pan, L. Zhu, X. Li, *Polym. Composite.* 34 (2013)1204.
- [20] M. Sethupathy, P. Pandey, P. Manisankar, *J. Appl. Polym. Sci.* DOI: 10.1002/app.41107
- [21] T. He, W. Zhou, A. Bahi, H. Yang, F. Ko, *Chem. Engin. J.* 252 (2014) 327.
- [22] L.Xu, M. Rungta, M.K. Brayden, M.V. Martinez, B.A. Stears, G.A. Barbay, W.J. Koros, *J. Membr. Sci.* 423-424 (2012) 314.
- [23] C. Zhao, X. Xu, J. Chen, G. Wang, F. Yang, *Desalination.* 340 (2014) 59.
- [24] Y. Zhao, Z. Xu, M. Shan, C. Min, B. Zhou, Y. Li, B. Li, L. Liu, X. Qian, *Sep. Purif. Technol.* 103(2013)78.
- [25] E.-S.Lee, D. Lei, K. Devarayan, B.-S. Kim. *Compos. Sci. Technol.*, 2015, 110, 111-117.

- [26] M.Grala, Z. Bartczak. *Polym. Eng. Sci.*, DOI: 10.1002/pen.24048
- [27] F. Li, T.-S. Chung, S. Kawi. *J. Membr. Sci.* 356 (2010) 14.
- [28] R. Hany, R. Hartmann, C. Böhlen, S. Brandenberger, J. Kawada, C. Löwe, M. Zinn, B. Witholt, R. H. Marchessault, *Polymer* 46(2005)5025.
- [29] Y.-J. Lee, J.-M. Huang, S.-W. Kuo, J.-S. Lu, F.-C. Chang. *Polymer* 46 (2005) 173.
- [30] J. Choi, J. Harcup, A. F. Yee, Q. Zhu, R. M. Laine. *J. Am. Chem. Soc.* 123(2001)11420.
- [31] J. P. Lewicki, K. Pielichowski, M. Jancia, E. Hebda, R.L.F. Albo, R. S. Maxwell, *Polym. Degrad. Stabil.* 104 (2014) 50.
- [32] J.H. Moon, A. R. Katha, S. Pandian, S. M. Kolake, S. Han, *J. Membr. Sci.* 461 (2014) 89.
- [33] F.-J. Fu, S. Zhang, S.-P. Sun, K.-Y. Wang, T.-S. Chung, *J. Membr. Sci.* 443 (2013) 144.
- [34] G. Tishchenko, M. Bleha, *J. Membr. Sci.* 248 (2005) 45.
- [35] S.C. Chen, X. Z. Fu, T.-S. Chung, *Desalination* 335 (2014) 17.
- [36] R. Konietzny, T. Koschine, K.Rätzke, C.Staudt, *Sep. Purif. Technol.* 123 (2014) 175.
- [37] D.-G. Kim, J. Shim, J. H. Lee, S.-J. Kwon, J.-H. Baik, J.-C. Lee, *Polymer* 54 (2013) 5812.
- [38] C.-H Jung, I.-T Hwang, C.-H Jung, J.-H Choi, *Radiat. Phys. Chem.* 102 (2014) 23.
- [39] J. Wu, Q. Ge, P.T. Mather, *Macromolecules* 43 (2010) 7637.
- [40] F. Wang, N. Phonthammachai, K.Y. Mya, W.W. Tjiu, C. He, *Chem. Commun.* 47 (2011) 767.
- [41] Kim, K.-O., Kim, B.-S., Lee, K.-H., Park, Y.-H., Kim, I.-S. *J. Mater. Sci.: Materials in Medicine* 24 (2013) 2029.
- [42] M.M. Rahman, V. Filiz, S. Shishatskiy, C. Abetz, S. Neumann, S. Bolmer, M.M. Khan, V. Abetz, *J. Membr. Sci.* 437 (2013) 286.
- [43] M.M. Rahman, S. Shishatskiy, C. Abetz, P. Georgopoulos, S. Neumann, M.M. Khan, V. Filiz, V. Abetz, *J. Membr. Sci.* 469 (2014) 344.
- [44] O. Suzuki, K. Watanabe. *Drugs and Poisons in Humans*, 2005, New York, Springer-Verlag Berlin Heidelberg, p 449.
- [45] L. Ye, D. Liu, H. Yu, *Membr. Sci. Technol.*, 1983, 3, 54-62.
- [46] L. Liu, H. Chen, F. Yang, *Sep. Purif. Technol.* 133 (2014) 22.
- [47] H.-P. Xu, W.-Z. Lang, X. Yan, X. Zhang, Y.-J. Guo, *J. Membr. Sci.* 467 (2014) 142.
- [48] X. Li, X. Lu. *J. Appl. Polym. Sci.* 101 (2006) 2944.

Figure caption list

1. Table 1 Elemental content of Epoxy-POSS and EG-POSS
2. Table 2 Crystallinity of hybrid membranes embedded with different EG-POSS content
3. Table 3 Roughness parameters of PVDF/EG-POSS hybrid membranes embedded with different EG-POSS content
4. Fig.1 NMR of OvPOSS and Epoxy-POSS
5. Fig. 2 FTIR spectra of OVPOSS, Epoxy-POSS and EG-POSS
6. Fig. 3 TEM micrographs of OvPOSS (A) and EG-POSS (B)
7. Fig.4 SEM micrographs of cross-section of PVDF/EG-POSS hybrid membranes embedded with different EG-POSS content (EG-POSS content: A: 0, B: 0.5%, C: 1.0%)
8. Fig.5 SEM micrographs of top surface (A1, B1, C) and bottom surface (A2, B2, C2) of PVDF/EG-POSS hybrid membranes embedded with different EG-POSS content (EG-POSS content: A: 0, B: 0.5%, C: 1.0%)
9. Fig.6 XRD patterns of PVDF/EG-POSS hybrid membranes embedded with different EG-POSS content
10. Fig.7 AFM images of PVDF/EG-POSS hybrid membranes embedded with different EG-POSS content
The content of EG-POSS is 0 (A), 0.5 (B) and 1.0 (C) respectively.
11. Fig.8 AFM images of the cross section of PVDF/EG-POSS hybrid membranes embedded with different EG-POSS content
The content of EG-POSS is 0 (A), 0.5 (B) and 1.0 (C) respectively.
12. Fig.9 Pure water flux and retention ratio of EG-POSS hybrid membranes embedded with different EG-POSS content
13. Fig.10 Contact angle of PVDF/EG-POSS hybrid membranes embedded with different EG-POSS content
14. Fig.11 Porosity (A), mean pore size (B) and shrinkage ratio (C) of PVDF/EG-POSS hybrid membranes embedded with different EG-POSS content
15. Fig.12 BSA adsorption capacity of PVDF/EG-POSS hybrid membranes embedded with different EG-POSS content
16. Fig.13 Mechanical property of PVDF/EG-POSS hybrid membranes embedded with different

EG-POSS content

17. Fig. 14 Tensile stress-strain curves of PVDF/EG-POSS hybrid membranes embedded with different EG-POSS content

Table 1 Elemental content of Epoxy-POSS and EG-POSS

Sample \ Element	C (%)	H (%)	N (%)
Epoxy-POSS	27.44	3.63	≤0.05
EG-POSS	18.79	3.86	≤0.05

Table 2 Crystallinity of hybrid membranes embedded with different EG-POSS content

Content of EG-POSS (%)	0	0.2	0.5	1.0	1.5	2.0
Crystallinity of hybrid membrane (%)	15.8	15.4	15.2	15.0	14.6	13.0

Table 3 Roughness parameters of PVDF/EG-POSS hybrid membranes embedded with different EG-POSS content

Content of EG-POSS (%)	0	0.5	1.0
Ra (nm)	86.97	87.76	75.04
Rq (nm)	111.65	106.67	91.33
Rmax (nm)	661.42	655.03	517.51

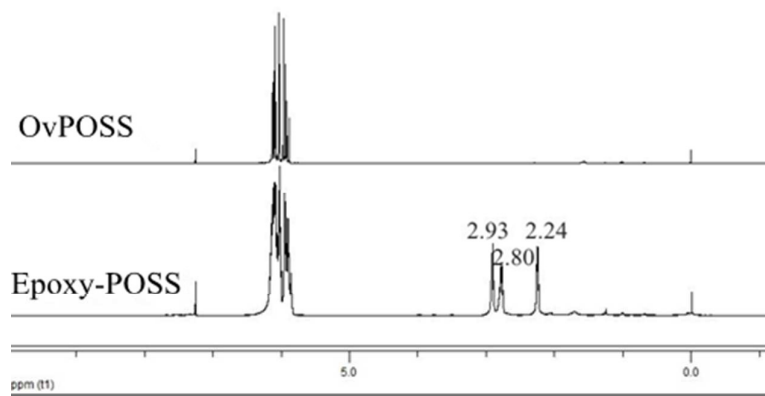


Fig.1 NMR of OvPOSS and Epoxy-POSS

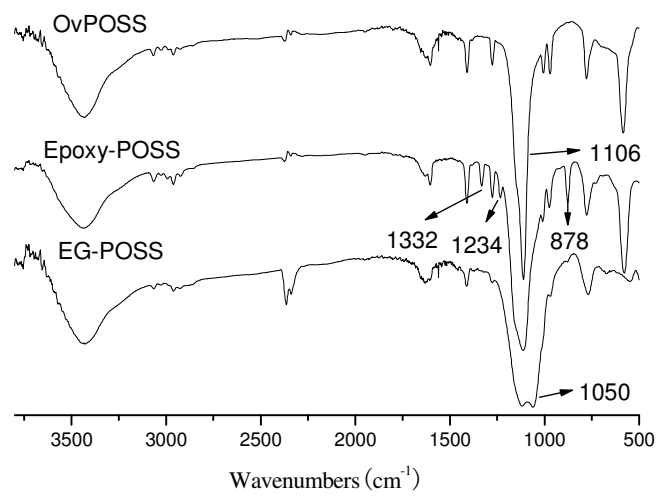


Fig. 2 FTIR spectra of OvPOSS, Epoxy-POSS and EG-POSS

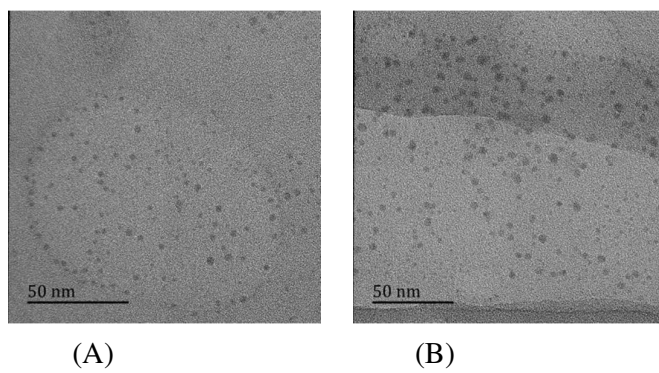


Fig. 3 TEM micrographs of OvPOSS (A) and EG-POSS (B)

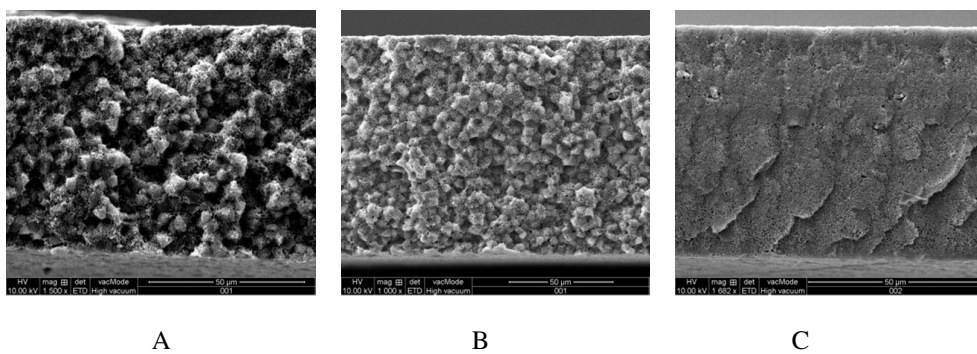


Fig.4 SEM micrographs of cross-section of PVDF/EG-POSS hybrid membranes embedded with different EG-POSS content (EG-POSS content: A: 0, B: 0.5%, C: 1.0%)

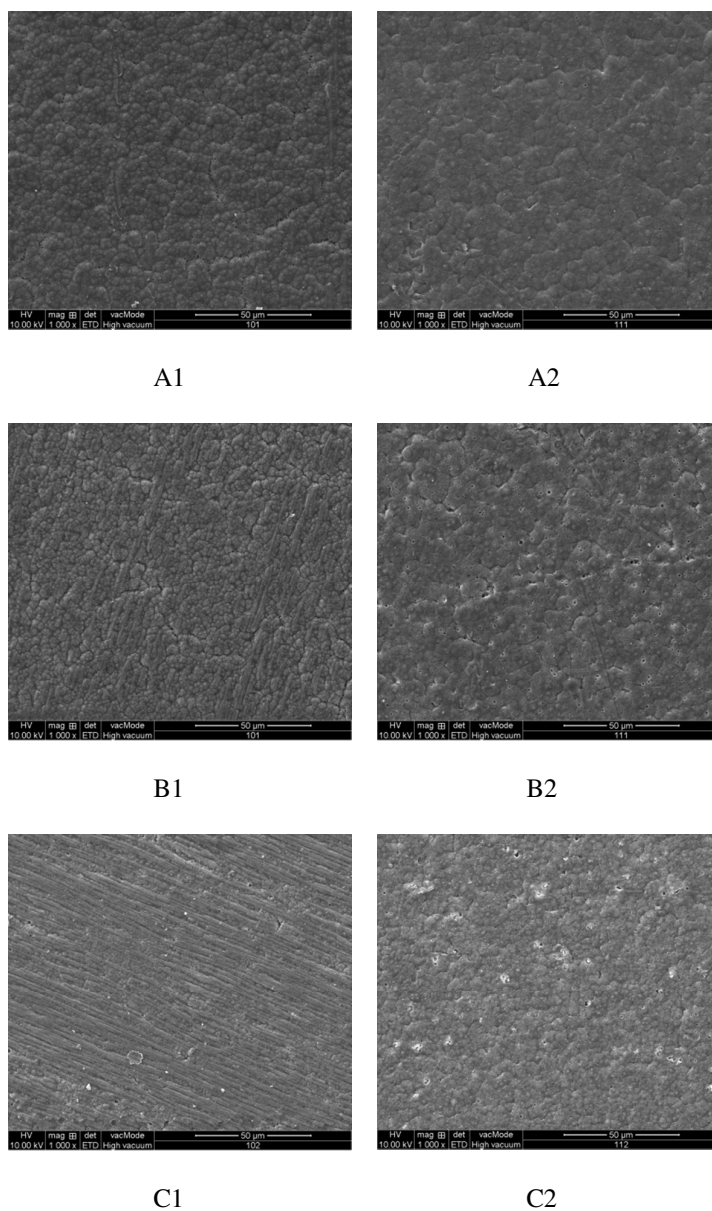


Fig.5 SEM micrographs of top surface (A1, B1, C1) and bottom surface (A2, B2, C2) of PVDF/EG-POSS hybrid membranes embedded with different EG-POSS content (EG-POSS content: A: 0, B: 0.5%, C: 1.0%)

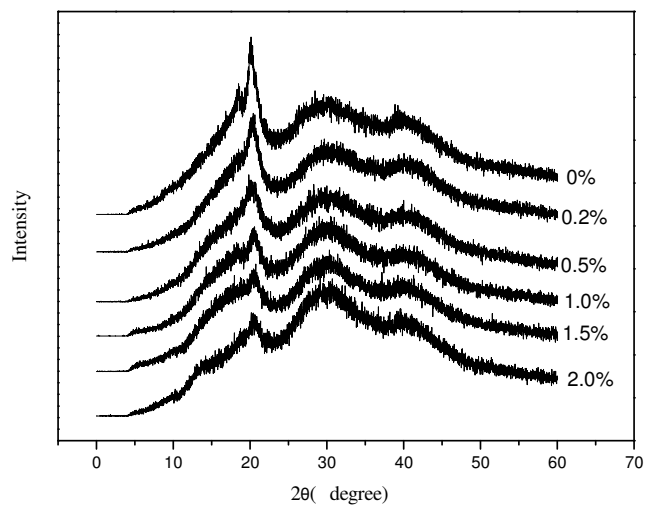


Fig. 6 XRD patterns of PVDF/EG-POSS hybrid membranes embedded with different EG-POSS content

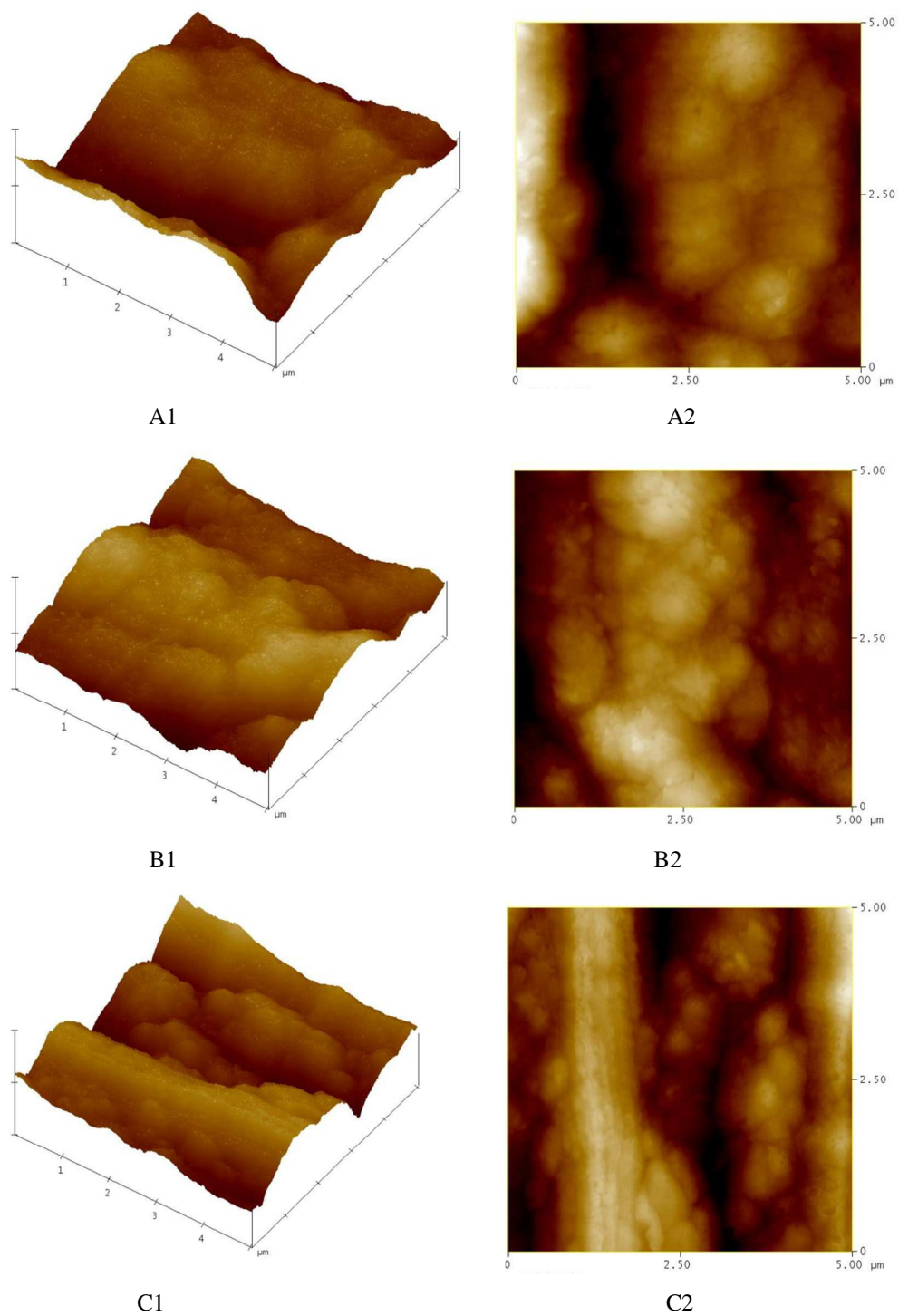


Fig. 7 AFM images of PVDF/EG-POSS hybrid membranes embedded with different EG-POSS content

The content of EG-POSS is 0 (A), 0.5 (B) and 1.0 (C) respectively.

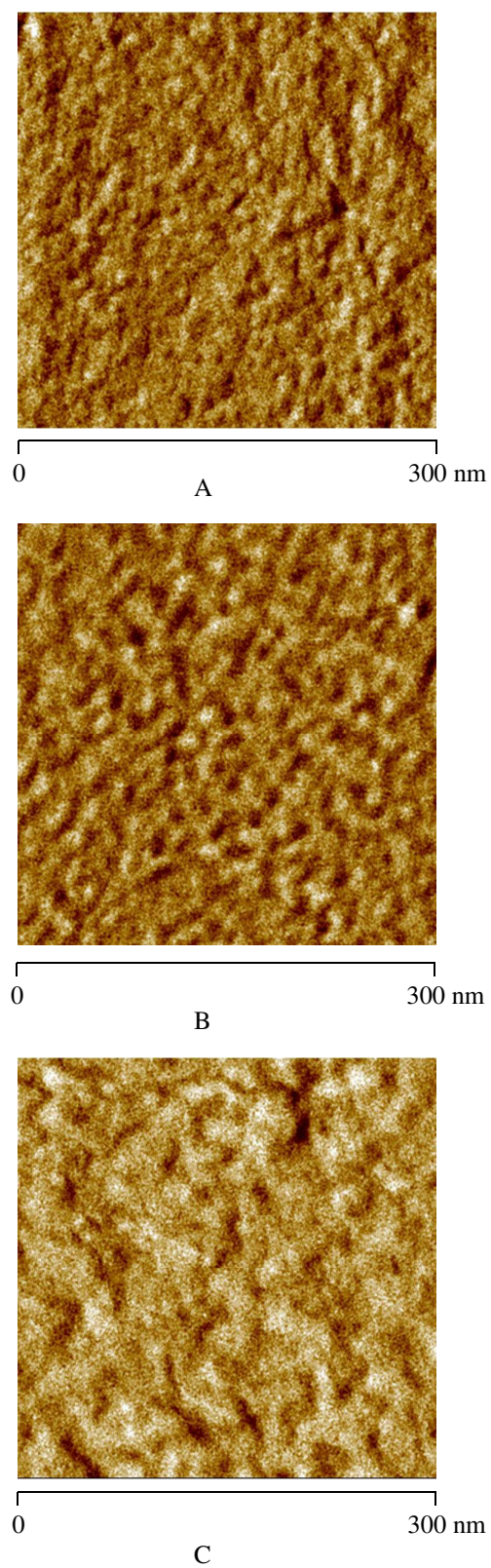


Fig. 8 AFM images of the cross section of PVDF/EG-POSS hybrid membranes embedded with different EG-POSS content

The content of EG-POSS is 0 (A), 0.5 (B) and 1.0 (C) respectively.

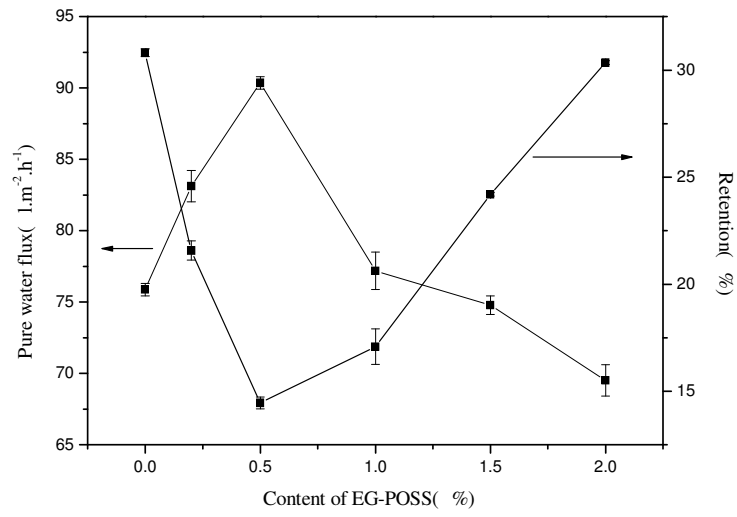


Fig. 9 Pure water flux and retention ratio of PVDF/EG-POSS hybrid membranes embedded with different EG-POSS content

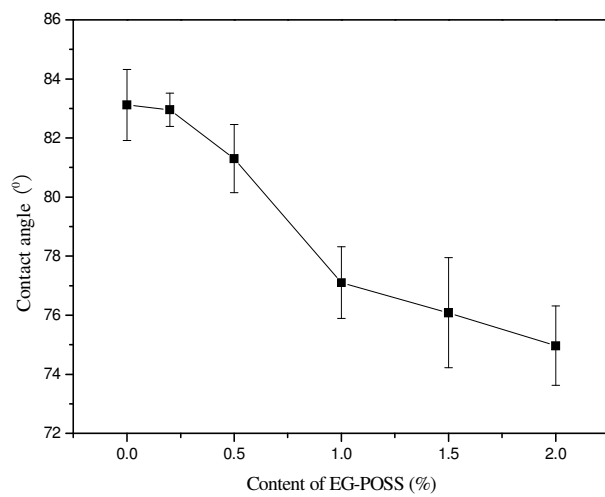
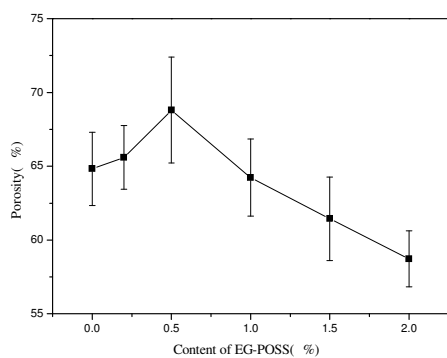
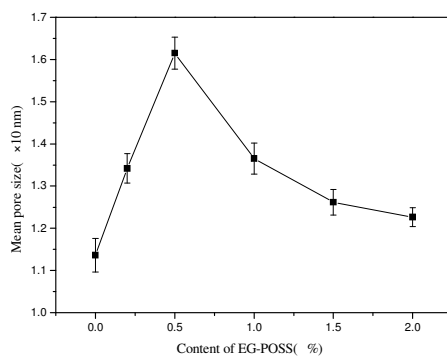


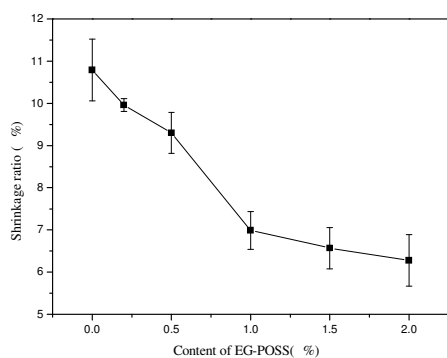
Fig. 10 Contact angle of PVDF/EG-POSS hybrid membranes embedded with different EG-POSS content



(A)



(B)



(C)

Fig. 11 Porosity (A), mean pore size (B) and shrinkage ratio (C) of PVDF/EG-POSS hybrid membranes embedded with different EG-POSS content

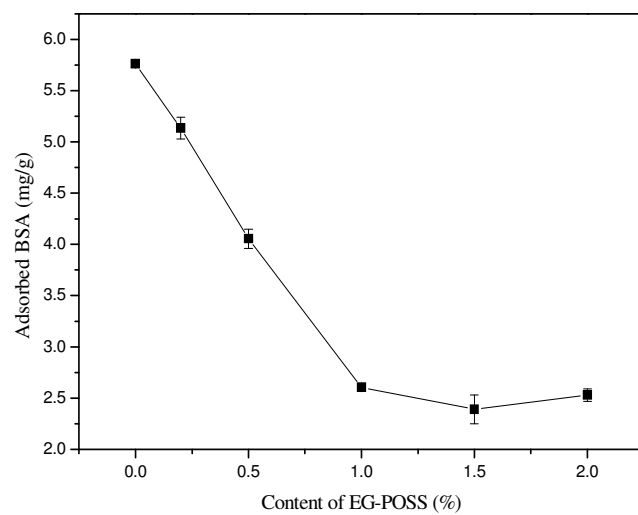


Fig. 12 Adsorption capacity of PVDF/EG-POSS hybrid membranes embedded with different EG-POSS content

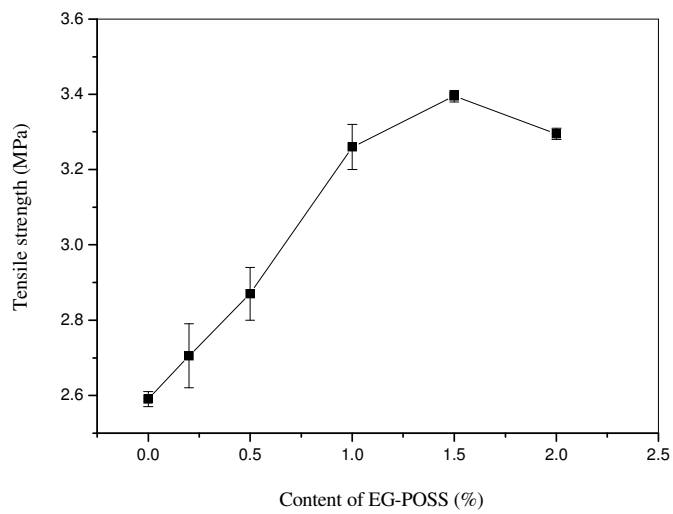


Fig.13 Mechanical property of PVDF/EG-POSS hybrid membranes embedded with different EG-POSS content

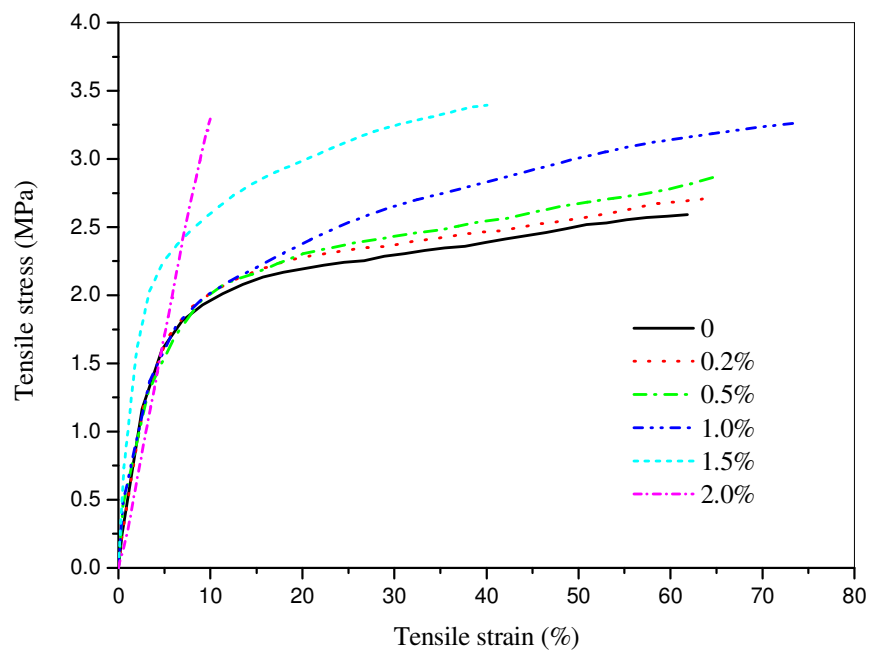


Fig. 14 Tensile stress-strain curves of PVDF/EG-POSS hybrid membranes embedded with different EG-POSS content